Biochemical and Biophysical Research Communications 434 (2013) 124–130

Contents lists available at SciVerse ScienceDirect

Biochemical and Biophysical Research Communications

journal homepage: www.elsevier.com/locate/ybbrc

Extracellular heat shock protein A9 is a novel interaction partner of podoplanin in oral squamous cell carcinoma cells

Masayuki Tsuneki [a,1], Satoshi Maruyama [b], Manabu Yamazaki [a], Bo Xu [c], Ahmed Essa [a], Tatsuya Abé [a,b], Hamzah Babkair [a], Jun Cheng [a], Tadashi Yamamoto [c], Takashi Saku [a,b,*]

[a] Division of Oral Pathology, Department of Tissue Regeneration and Reconstruction, Niigata University Graduate School of Medical and Dental Sciences, Niigata, Japan
[b] Oral Pathology Section, Department of Surgical Pathology, Niigata University Hospital, Niigata, Japan
[c] Department of Structural Pathology, Institute of Nephrology, Niigata University Graduate School of Medical and Dental Sciences, Niigata, Japan

ARTICLE INFO

Article history:
Received 4 March 2013
Available online 26 March 2013

Keywords:
Heat shock protein A9 (HSPA9)
Podoplanin
Podoplanin-binding protein
Proteomics
Oral squamous cell carcinoma

ABSTRACT

In previous studies, we have shown several lines of evidence that podoplanin (PDPN) plays an important role in cell adhesion via its association with extracellular components in neoplastic conditions, though there has been no trial to search for PDPN-interaction molecules in the extracellular milieu. To screen for those molecules, we performed proteomics-based analysis using liquid chromatography-tandem mass spectrometry followed by co-immunoprecipitation for PDPN in ZK-1, an oral squamous cell carcinoma (SCC) cell system whose cell membrane molecules were cross-linked with each other in their extracellular compartments, and we identified heat shock protein (HSP) A9 as one of the extracellular PDPN bound molecules. Effects of transient PDPN knockdown by siRNA in ZK-1 were also comparatively examined for cellular behaviors in terms of HSPA9 expression and secretion. Finally, HSPA9 expression modes were immunohistochemically visualized in oral SCC tissue specimens. HSPA9 was secreted from ZK-1 cells, and the expression and secretion levels of HSPA9 gene and protein were well coordinated with those of PDPN. Immunohistochemically, HSPA9 and PDPN were co-localized in ZK-1 cells and oral SCC foci, especially in the peripheral zone. In conclusion, the results indicate that HSPA9 secreted by oral SCC cells interacts with PDPN on their cell surface in an autocrine manner and regulates their growth and invasiveness.

1. Introduction

Podoplanin (PDPN), a mucin-type transmembrane sialoglycoprotein, was originally identified in glomerular visceral epithelial cells (podocytes) [1] and has been utilized as one of the most representative markers of lymphatic endothelium [2]. In recent years, PDPN expression in parenchymal cells has been confirmed in various kinds of benign and malignant tumors such as thymoma [3], central nervous system germ cell tumors [4], and lung squamous cell carcinoma (SCC) [5]. We have also revealed the characteristic immunolocalization of PDPN in close association with neoplastic stromata in oral epithelial dysplasia, carcinoma in situ and SCC [6,7], as well as in salivary gland tumors [8] and odontogenic tumors [9]. In addition, we demonstrated that PDPN tethers oral SCC cells to hyaluronan-rich extracellular matrices in collaboration with CD44 and hence suggested the function of PDPN in communication with extracellular matrix (ECM) elements [7]. Based on the results from our latest investigation, it was necessary for us to identify any possible candidate molecules which interact with PDPN at its extracellular compartment.

The extracellular domain of PDPN, which is rich in Ser and Thr, contains multiple potential *O*-glycosylation sites [10]. C-type lectin-like receptor 2 (CLEC-2) [11], galectin-8 [12], and CD44 [13] have been shown to interact with PDPN at the extracellular domain in different cellular events like tumor cell-induced platelet aggregation [11], lymphatic endothelial cell adhesion [12], and directional tumor cell migration [13]. However, these are cell membrane molecules which have not originated from the ECM side. The purpose of the present study was to search for PDPN-interacting molecules by means of proteomics-based analysis and confirm ECM interaction using the same oral SCC cell system which was used in our recent study [7].

2. Materials and methods

2.1. Cell systems and reagents

The oral SCC cell system (ZK-1) was established from SCC arising in the tongue [15]. ZK-1 cells were cultured in Dulbecco's modified Eagle medium (DMEM) (Gibco, Invitrogen Corporation,

* Corresponding author. Address: Division of Oral Pathology, Department of Tissue Regeneration and Reconstruction, Niigata University Graduate School of Medical and Dental Sciences, 2-5274 Gakkocho-dori, Chuo-ku, Niigata 951-8514, Japan. Fax: +81 25 227 0805.
E-mail address: tsaku@dent.niigata-u.ac.jp (T. Saku).
[1] Fellow, the Japan Society for the Promotion of Science, Japan.

0006-291X/$ - see front matter © 2013 Elsevier Inc. All rights reserved.
http://dx.doi.org/10.1016/j.bbrc.2013.03.057

Carlsbad, CA, USA) containing 10% fetal bovine serum (FBS) (Gibco), 50 μg/ml streptomycin, and 50 IU/ml penicillin (Gibco) [7]. They were incubated at 37 °C in a humidified 5% carbon dioxide/95% air atmosphere.

2.2. Antibodies

A mouse monoclonal antibody against human PDPN (D2-40, IgG_1) was obtained from Dako (Glostrup, Denmark). Rabbit polyclonal antibodies to human HSPA9 (Grp75) and ezrin and a mouse monoclonal antibody to human β-actin (mAbcam 8226, IgG_1) were purchased from Abcam plc. (Cambridge, UK). Mouse and rabbit preimmune IgGs for control experiments were also obtained from Dako.

2.3. Immunoprecipitation and silver staining

For immunoprecipitation, ZK-1 cells (1.0×10^5 cells/60 mm dish) were cultivated for 72 h and lysed in lysis buffer (50 mM HEPES pH 7.4, 150 mM NaCl, 1.0% Brij-96, 1 mM PMSF, 1 mM Na_3VO_4, and 10 mM NaF) containing a protease inhibitor cocktail (Nacalai Tesque, Kyoto, Japan). After incubation of 1 mg of cell lysates for 2 h at 4 °C with 5 μg of anti-PDPN antibodies or preimmune IgG, 70 μl of 50% slurry of Protein G Sepharose™ 4 Fast Flow (GE Healthcare UK Ltd., Buckinghamshire, UK) were added to each sample and stirred for 2 h at 4 °C. After incubation, the protein G Sepharose resin was washed 3 times with lysis buffer and then 2 times with final buffer (50 mM HEPES pH 7.4, 150 mM NaCl). The immunoprecipitates were eluted in 50 μl of 2× SDS sample buffer containing 10% β-mercaptoethanol. An aliquot of 20 μl of elution sample was subjected to SDS polyacrylamide gel electrophoresis (SDS–PAGE) under reducing condition, and the gels were stained using a Bio-Rad Silver Stain kit (Bio-Rad Laboratories, Inc., Hercules, CA, USA) or transferred to polyvinylidene difluoride (PVDF) membranes (Bio-Rad) for Western blotting.

2.4. Western blotting

After incubation with 0.5% enhanced chemiluminescence (ECL) blocking agent (GE Healthcare UK Ltd., Buckinghamshire, UK) in 50 mM Tris-buffered saline (TBS) (pH 7.4) containing 0.1% Tween-20 (TTBS) for 1 h at room temperature, the PVDF membranes were further incubated overnight at 4 °C with primary antibodies diluted with TTBS (PDPN, 1:100; HSPA9 and ezrin, 1:1000; β-actin, 1:5000), followed by secondary antibodies (ChemMate Envision™ reagent, Dako, diluted at 1:1000 in TTBS) for 1 h at room temperature [8]. Target protein bands were visualized by ECL Plus™ Western blotting detection reagents (GE).

2.5. Proteome analysis

Candidate PDPN-interacting protein SDS–PAGE gel bands were excised and in-gel digested with trypsin as described elsewhere [16]. The digest mixtures were separated and analyzed by a nano-flow-liquid chromatography-tandem mass spectrometer (Agilent 1100 LC/MSD Trap XCT) (Agilent Technologies, Inc., Santa Clara, CA, USA). The data were searched against a NCBI non-redundant database with MASCOT MS/MS Ions Search (Matrix Science Inc., Boston, MA, USA).

2.6. Cell surface protein interaction

To confirm the extracellular cell surface interaction between PDPN and HSPA9, we performed extracellular cross-linking using DTSSP (3,3′-dithiobis[sulfosuccinimidylpropionate]) (Pierce Biotechnology, Rockford, IL, USA) [17]. ZK-1 cells (1.0×10^5 cells/60 mm dish) were cultivated for 72 h and washed twice with washing buffer (50 mM HEPES pH 7.4, 150 mM NaCl). After incubation for 2 h on ice with 5 ml of DTSSP cross-linking solution (1 mM DTSSP, 50 mM HEPES pH 7.4, 150 mM NaCl), we added 50 μl of 1 M Tris–HCl (pH 7.5) to stop cross-linking reaction. Thereafter, immunoprecipitation for anti-PDPN or anti-HSPA9 was performed as mentioned above following cytolysis to demonstrate protein complex bands [17].

2.7. RNA interference (RNAi)

RNAi experiments were performed using a Stealth RNAi™ siRNA Duplex Oligoribonucleotides System (Invitrogen). The human PDPN siRNA (siPDPN) sequence used in this experiment was 5′-UGAAG UUGGC AGAUC CUCGA UGCGA-3′, which was shown to be the most effective in our previous experiments [7]. Stealth RNAi™ negative control medium GC Duplex #2 (Invitrogen) (siNC) and sterile Milli-Q™ water (mock) were used as negative controls. siRNA transfection was performed with Lipofectamine RNAiMAX™ reagents (Invitrogen). Efficiencies for RNAi were evaluated using real-time PCR, Western blotting, and immunofluorescence.

2.8. Gene and protein expression analysis

Total RNA was isolated from the cells, which were plated at a concentration of 1.0×10^5 cells/60 mm dish and cultivated for 72 h using the ISOGEN system (Nippon Gene Co., Ltd., Tokyo, Japan). First strand cDNA was synthesized with the SuperScript™ III First-Strand Synthesis System (Invitrogen). Following reverse transcription, real-time PCR was carried out using a MiniOpticon™ Real-Time PCR Detection System CFB-3120 (Bio-Rad Laboratories, Inc., Hercules, CA, USA). Amplification of target genes was monitored in real time, and gene expression levels were quantified using CFX Manager™ (Bio-Rad). Primer sets used for the real-time PCR experiments are summarized in Table 1. For each gene, protein expression was also demonstrated by Western blotting and analyzed quantitatively using NIH Image J computer-assisted densitometric image analysis software.

2.9. Quantitative secretion analysis

To determine HSPA9 secretion from with or without siRNA transfected ZK-1 cells (siPDPN, siNC, and mock), 1.0×10^5 cells/60 mm dish were cultivated for 72 h and supernatant fluid of cultured medium was collected. After immunoprecipitation against HSPA9 antibodies, secretory HSPA9 protein band was detected by Western blotting and analyzed using NIH Image J.

2.10. Immunofluorescence

Immunofluorescence experiments were performed using Lab-Tek™ II Chamber Slide System (Labtek, Scotts Valley, CA, USA) as

Table 1
Primer sequences for quantification of gene expression.

Gene	Primer sequence
Human PDPN	F: 5′-CCAAGCGCCACAGCCTCAA-3′
	R: 5′-GGCACAGAGTCAGAAACGGT-3′
Human HSPA9	F: 5′-AGCTGGAATGGCCTTAGTCAT-3′
	R: 5′-CAGGAGTTGGTAGTACCCAAATC-3′
Human ezrin	F: 5′-GCTTTTTGATCAGGTGGTAAAGACT-3′
	R: 5′-TCCACATAGTGGAGGCCAAAGT-3′
Human β-actin	F: 5′-TCACCCACACTGTGCCCATCTACGA-3′
	R: 5′-CAGCGGAACCGCTCATTGCCAATGG-3′

F: forward; R: reverse.

described elsewhere [15]. Cells were plated at a concentration of 1.0×10^4 cells/well and cultivated for 72 h. The cells were treated under the four experimental conditions, with or without DTSSP cross-linking (CL) and 0.2% Triton X-100 cell membrane permeabilization (TrX), as follows: CL(+), TrX(+); CL(+), TrX(−); CL(−), TrX(+); CL(−), TrX(−). For CL(+), cell surface molecules were cross-linked by DTSSP as mentioned above (section of cell surface protein interaction) and fixed with 4% paraformaldehyde in 0.1 M HEPES (pH 7.4) for 30 min on ice. The cells were incubated with the primary antibodies (PDPN, diluted at 1:50 in reaction buffer; HSPA9, 1:500) and further with secondary antibodies (Alexa Fluor™ 568-conjugated goat anti-mouse IgG (H + L) or Alexa Fluor™ 488-conjugated goat anti-rabbit IgG (H + L) (Invitrogen), diluted at 1:200 reaction buffer for 1 h each at room temperature. For control studies, the primary antibodies were replaced with preimmune mouse or rabbit IgGs.

2.11. Surgical samples

Fifteen cases of oral SCC were collected from the surgical pathology files of the Division of Oral Pathology, Niigata University Graduate School of Medical and Dental Sciences. The surgical samples were fixed in 10% formalin, processed routinely, and embedded in paraffin. Serial sections cut at 4 μm from paraffin blocks were used for haematoxylin and eosin (H–E) staining and immunohistochemistry.

2.12. Immunohistochemistry

Immunohistochemistry was performed using the ChemMate Envision™ system (Dako) as described elsewhere [18]. The sections were incubated overnight at 4 °C with the primary antibodies diluted at 1:50 (anti-PDPN) and 1:1000 (anti-HSPA9) in PBS. After incubation with the Envision™ reagents, reaction products were developed with SIGMAFAST™ DAB/Metal Enhancer Tablet Set (Sigma Chemical Co., Saint Louis, MO, USA). For control studies, the primary antibodies were replaced with preimmune IgGs. The experimental protocol for analyzing surgical materials was reviewed and approved by the Ethical Board of the Niigata University School of Dentistry.

2.13. Statistical analysis

Comparative experimental data were analyzed using the *t*-test. The cut-off for statistical significance was set at $P < 0.05$. All statistical analyses were carried out using the SigmaPlot 2001 for Windows version 7.0 (SPSS Inc., Chicago, IL, USA) and Microsoft Excel 2007.

3. Results

3.1. Identification of HSPA9 as a candidate interacting molecule with PDPN

To identify novel interacting proteins of human PDPN in oral SCC, we performed immunoprecipitation using ZK-1 cells which endogenously express PDPN [7]. We found a protein band with a Mr mass of 70 kDa in SDS–PAGE gels stained with silver impregnation (Fig. 1(A), left panel, asterisk) among those co-immunoprecipitated with PDPN. Western blotting with anti-PDPN antibody confirmed that the protein was not a variant of PDPN (Fig. 1(A), right panel). The 70 kDa band was identified to be HSPA9 by nano-flow LC–MS/MS analysis. Detailed data on LC–MS/MS analysis were as follows: number of distinct peptides, 17; distinct summed MS/MS search score, 230.28; amino acid (AA) coverage, 26%; mean peptide spectral intensity, 1.61E+07; database accession number, IPI00007765.

3.2. Interaction between HSPA9 and PDPN on the cell surface

Western blotting with the anti-HSPA9 antibody confirmed that the 70 kDa band of HSPA9 was again co-immunoprecipitated with PDPN (Fig. 1(B)). Because subcellular localization of PDPN had already been identified on the cell membrane [7], cross-linking co-immunoprecipitation in the presence of DTSSP was performed to confirm the extracellular cell surface interaction between HSPA9

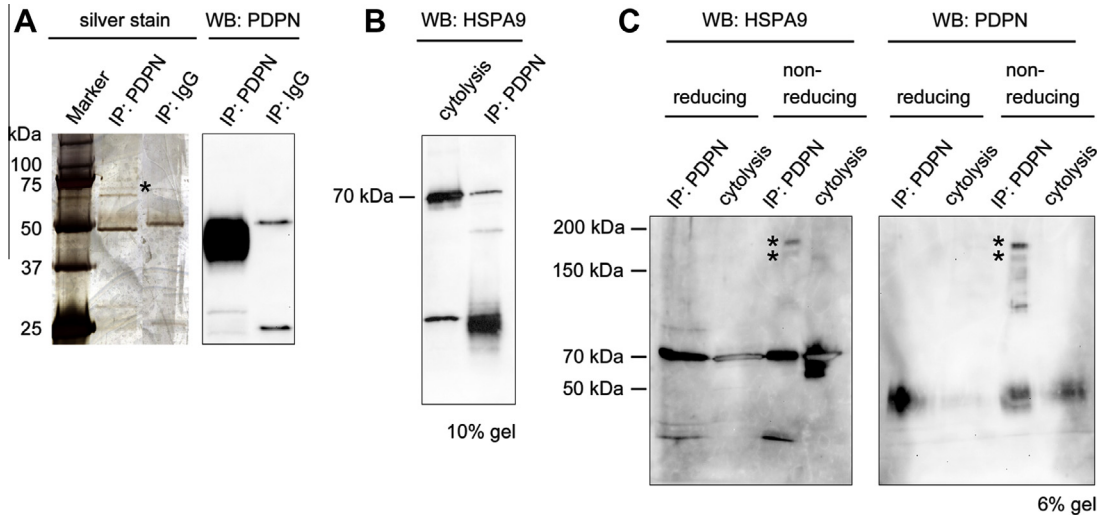

Fig. 1. Identification of heat shock protein A9 (HSPA9) as a novel interaction partner for podoplanin (PDPN) in the cell surface. (A) ZK-1 cell lysates were immunoprecipitated with anti-human PDPN antibody (IP: PDPN) or control mouse IgG (IP: IgG), followed by sodium dodecyl sulfate–polyacrylamide gel electrophoresis (SDS–PAGE) with silver staining (left panel) and Western blotting for PDPN (right panel); (B) Western blotting analysis for HSPA9 (70 kDa) in cell lysates (cytolysis, left lane) and in its immunoprecipitated samples with the anti-PDPN (IP: PDPN, right lane), 10% SDS–gel. (C) Western blot analyses for HSPA9 (left panel) or PDPN (right panel) in immunoprecipitated samples of lysates from ZK-1 cells cross-linked with DTSSP with the anti- PDPN, 6% SDS–polyacrylamide gel. A protein band (asterisk in left panel) at around 70 kDa was detected as a possible PDPN-binding partner protein (A). Mass spectrometric analysis (LC–MS/MS) of the protein band obtained from silver stained gels identified it as heat shock protein (HSP) A9. Western blotting showed that HSPA9 was co-precipitated with PDPN (B). PDPN and HSPA9 were demonstrated to co-localized on the cell surface because bands indicating the PDPN–HSPA9 complex were detected around 150–180 kDa (asterisks) in non-reducing conditions (C).

and PDPN. HSPA9–PDPN interacting complex bands were detected around 150–180 kDa areas (Fig. 1(C), asterisks), which were distinctly shifted from their original positions in the non-reducing conditions of SDS–PAGE and Western blotting (anti-HSPA9 and PDPN) (Fig. 1(C)).

3.3. Coordinated HSPA9 expression and secretion with PDPN

Based on the finding that HSPA9 was bound to PDPN, we sought to determine whether expression and secretion modes of HSPA9 were coordinated with those of PDPN in an effective PDPN knock-down experimental system using siRNA in ZK-1 cells, which we had already established [7]. PDPN was significantly suppressed in siPDPN cells at 72 h after plating (down to 7% of controls, $P < 0.001$) (Fig. 2(A)). Coincidental with the suppressed expression of PDPN, gene (Fig. 2(B), $P < 0.05$) and protein (Fig. 2(C), $P < 0.01$) expression levels for HSPA9 were lowered in siPDPN cells. In contrast, the expression of ezrin, a cytoplasmic peripheral membrane protein which has already been identified as a possible interacting protein with PDPN [19], was not altered in siPDPN cells at either the gene or the protein level. When detected by immunoprecipitation, secreted HSPA9 protein levels were significantly repressed in siPDPN cells (Fig. 2(E), $P < 0.001$, Fig. 2(F)).

3.4. Harmonized expression and localization of PDPN and HSPA9

To identify interlocked expression and colocalization of PDPN and HSPA9, we examined double-immunofluorescence and compared between siPDPN cells and siNC ZK-1 cells in the presence or absence of DTSSP cross-linking (CL) as well as with and without Triton X-100 cell membrane permeabilization (TrX) as follows: CL(+), TrX(+) (Fig. 3(A)); CL(−), TrX(+) (Fig. 3(B)); CL(−), TrX(−) (Fig. 3(C)); CL(+), TrX(−) (Fig. 3(D)). In all conditions, HSPA9 expression levels were suppressed and restricted to the periphery

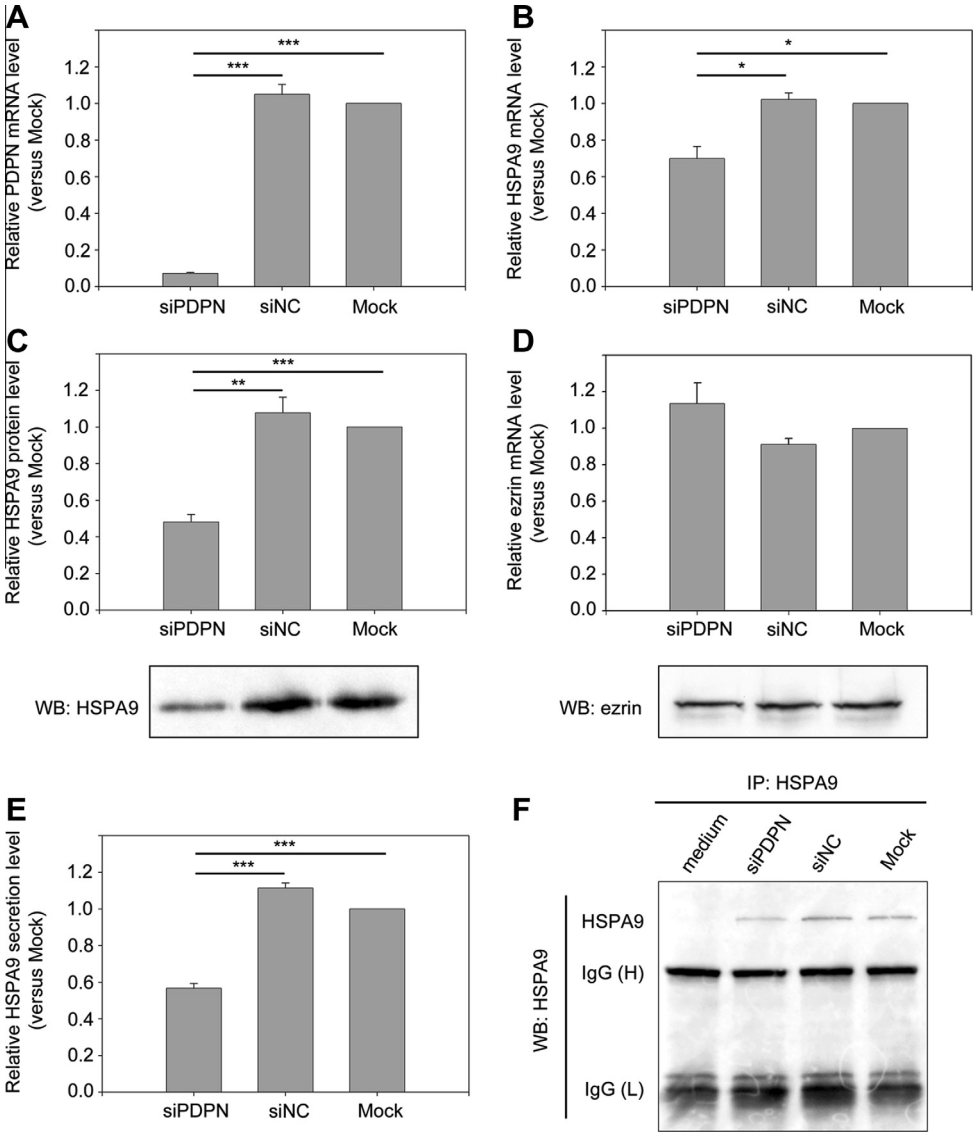

Fig. 2. HSPA9 association with PDPN in its expression and secretion. (A) Knock-down of PDPN by siRNA in ZK-1 cells. Relative PDPN gene expression levels determined by real-time PCR and compared between cells transfected by siRNA targeting PDPN (siPDPN), negative control siRNA (siNC), and mock; real-time PCR for HSPA9 gene (B) and Western blotting for HSPA9 protein (C) between siPDPN, siNC, and mock. (D) Ezrin gene and protein expression by real-time PCR (upper panel) and Western blotting (lower panel) between siPDPN, siNC, and mock; HSPA9 secretion levels by immunoprecipitation (E) and Western blotting HSPA9 (F) compared between culture media of siPDPN, siNC, and mock. (A–E) All data are means ± SE from triplicate experiments. $^{*}P < 0.05$; $^{**}P < 0.01$; $^{***}P < 0.001$.

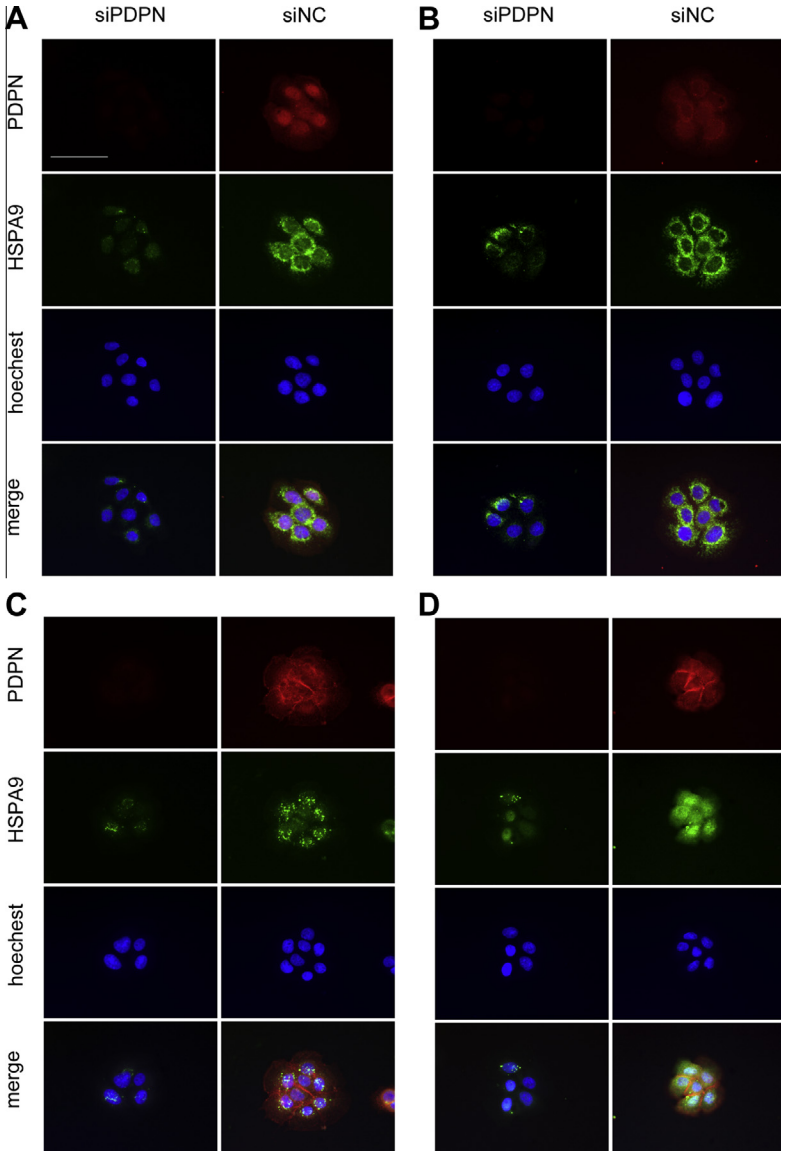

Fig. 3. Colocalization of PDPN and HSPA9 in the cell surface of ZK-1 cells. (A–D) Immunofluorescence for PDPN (red, upper row) and HSPA9 (green, second), Hoechst-33258 (blue, second from bottom), and their merges (bottom) compared between siPDPN (left column) and siNC (right column) in the combinations of DTSSP cross-linking (CL) and Triton X-100 cell membrane permeabilization (TrX) as follows: CL(+), TrX(+) (A); CL(−), TrX(+) (B); CL(−), TrX(−) (C); CL(+), TrX(−) (D). ×200; scale bar, 100 μm. (For interpretation of the references to color in this figure legend, the reader is referred to the web version of this article.)

of the nucleus in siPDPN cells (Fig. 3). After TrX membrane permeabilization, PDPN and HSPA9 were localized in the cytoplasm of siNC cells (Fig. 3(A) and (B)), while PDPN slightly remained on the cell membrane under CL conditions (Fig. 3(A)). In contrast, before permeabilization, PDPN and HSPA9 were colocalized on the cell membrane of siNC cells under CL conditions (Fig. 3(D)), whereas HSPA9 was not localized on the cell membrane but in the cytoplasm under non-CL conditions (Fig. 3(C)). Thus, HSPA9 was clearly shown to be expressed in coordination with PDPN and they were colocalized on the cell surface of ZK-1 cells.

To further investigate the coordinated expression profiles between PDPN and HSPA9 at the tissue level, we performed immunohistochemistry for PDPN and HSPA9 in surgical tissue sections of oral SCC. In the foci of SCC (Fig. 4(A)), PDPN was distinctively localized on the cell border as well as in the basal surface of peripheral cells (Fig. 4(B)), which were simultaneously positive for HSPA9 (Fig. 4(C)). Those co-localizations in the periphery of SCC foci were most enhanced in their invading front.

4. Discussion

In the present study, we demonstrated for the first time the extracellular shedding of HSPA9 from oral SCC cells. Secondly, by using cross-linking treatments [17], the interaction between HSPA9 and PDPN in the cell surface was confirmed. Thirdly, the gene and protein expression levels as well as the secretion levels of HSPA9 were specifically correlated with those of PDPN. Finally, the co-localization of HSPA9 and PDPN on the cell surface was also confirmed in surgical specimens of oral SCC.

PDPN has been utilized in the field of lymphatic research [2] as one of the representative lymphatic endothelial markers. Recently, PDPN expression has been documented in various kinds of tumor cells [3,6,20,21], and has attracted attention in the area of cancer research. In oral SCC, PDPN expression has been related to poor clinical outcomes, including nodal metastasis, as well as to malignant transformation of pre-cancerous lesions [22–24]. To elucidate the molecular function of PDPN, we have carried out comparative

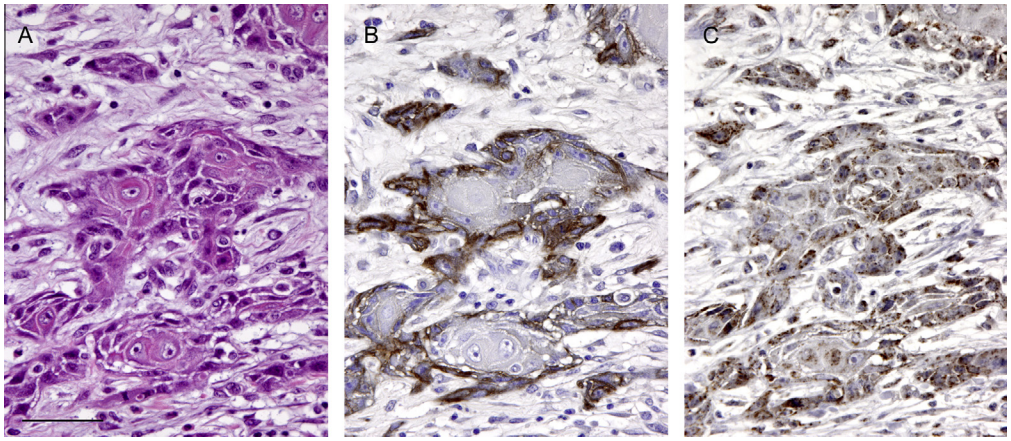

Fig. 4. Colocalization of PDPN and HSPA9 in the periphery of foci of oral squamous cell carcinoma (SCC). (A) Hematoxylin and eosin (HE) stain; immunoperoxidase stain for PDPN (B) and HSPA9 (C), hematoxylin counterstain. ×150; scale bar, 100 μm.

immunohistochemical studies and in vitro functional analysis in terms of cell-proliferation and ECM association because PDPN was characteristically localized in the tumor cell nest periphery, directly facing the stromal space which was rich in extracellular matrix [6–9,15,25]. From our series of investigation, we have concluded that PDPN tethers tumor cells to hyaluronan-rich extracellular matrices in collaboration with CD44 to inhibit cellular scattering [7,8]. In other words, PDPN contributes to cell-ECM adhesion but not directly to cell proliferation, which must be an event that is secondary to established cell adhesion [7–9]. Based on these lines of evidence, we have been focusing on interaction molecules with PDPN in their extracellular domain or cell surface.

To identify novel interacting proteins of PDPN, our strategy to introduce proteomics-based analysis using LC–MS/MS followed by co-immunoprecipitation was so successful that we were firstly able to identify HSPA9 as a novel PDPN-binding partner. We also detected ezrin in the co-immunoprecipitants (data not shown). Since it had already been known as an interaction molecule [19], it was regarded as a kind of positive control in this experimental system.

HSPA9 was first identified as a member of the 70 kDa heat shock protein (hsp70) family present in the cytoplasmic fractions of normal fibroblasts (MEF cells) from CD1-ICR mice [26]. It has also been cloned as a peptide binding protein (PBP74) [27], mitochondrial heat shock protein (mthsp70) [28], and glucose regulated protein (GRP75) [29]. Its multiple subcellular localizations, including in plasma membrane, have been reported [14]. The HSPA9 expression was up-regulated in human neoplasms [30] such as brain tumors [31], colorectal adenocarcinomas [32], hepatocellular carcinoma [33], and breast ductal carcinoma [34], and those enhanced expression levels were correlated with poor clinical outcomes [32,33]. Interestingly, HSPA9 was demonstrated to be released from cells to the extracellular space, though it lacks consensus secretory signal peptides within the molecule [35–37]. However, little is known about the HSPA9 behavior in the extracellular space.

In conclusion, we have identified HSPA9 as a novel PDPN binding partner in the cell surface. Since HSPA9 was secreted from ZK-1 cells, their binding should take place in an autocrine fashion. The characteristic PDPN immunolocalization in the periphery of SCC foci suggests its role in the SCC cell crosstalk with the stroma, which possibly regulates SCC cell activities for invasion. In the next step, it is necessary to elucidate detailed molecular functions of the HSPA9–PDPN complex on the cell surface, especially in terms of proliferation and invasion.

Acknowledgments

This work was supported in part by Grants-in-Aid for Scientific Research from the Japan Society for the Promotion of Science (JSPS) and for JSPS Fellows, with additional funding from the Iwadare Scholarship Foundation, Japan.

References

[1] S. Breiteneder-Geleff, K. Matsui, A. Soleiman, et al., Podoplanin, novel 43-kd membrane protein of glomerular epithelial cells, is down-regulated in puromycin nephrosis, Am. J. Pathol. 151 (1997) 1141–1152.
[2] S. Kundu, J. Cheng, S. Maruyama, et al., Lymphatic involvement in the histopathogenesis of mucous retention cyst, Pathol. Res. Pract. 203 (2007) 89–97.
[3] H. Tateyama, H. Sugiura, C. Yamatani, et al., Expression of podoplanin in thymoma: its correlation with tumor invasion, nodal metastasis, and poor clinical outcome, Hum. Pathol. 42 (2011) 533–540.
[4] K. Mishima, Y. Kato, M.K. Kaneko, et al., Podoplanin expression in primary central nervous system germ cell tumors: a useful histological marker for the diagnosis of germinoma, Acta Neuropathol. 111 (2006) 563–568.
[5] Y. Kato, M. Kaneko, M. Sata, et al., Enhanced expression of Aggrus (T1alpha/podoplanin), a platelet-aggregation-inducing factor in lung squamous cell carcinoma, Tumour. Biol. 26 (2005) 195–200.
[6] A. Funayama, J. Cheng, S. Maruyama, et al., Enhanced expression of podoplanin in oral carcinomas in situ and squamous cell carcinomas, Pathobiology 78 (2011) 171–180.
[7] M. Tsuneki, M. Yamazaki, S. Maruyama, et al., Cell adhesive function of podoplanin in oral squamous cell carcinoma, J. Oral. Biosci. 53 (2011) S125.
[8] M. Tsuneki, S. Maruyama, M. Yamazaki, et al., Podoplanin is a novel myoepithelial cell marker in pleomorphic adenoma and other salivary gland tumors with myoepithelial differentiation, Virchows Arch 462 (2013) 297–305.
[9] M. Tsuneki, S. Maruyama, M. Yamazaki, et al., Podoplanin expression profiles characteristic of odontogenic tumor-specific tissue architectures, Pathol. Res. Pract. 208 (2012) 140–146.
[10] M.K. Kaneko, Y. Kato, A. Kameyama, et al., Functional glycosylation of human podoplanin: glycan structure of platelet aggregation-inducing factor, FEBS. Lett. 581 (2007) 331–336.
[11] K. Suzuki-Inoue, Y. Kato, O. Inoue, et al., Involvement of the snake toxin receptor CLEC-2, in podoplanin-mediated platelet activation, by cancer cells, J. Biol. Chem. 282 (2007) 25993–26001.
[12] L.N. Cueni, M. Detmar, Galectin-8 interacts with podoplanin and modulates lymphatic endothelial cell functions, Exp. Cell. Res. 315 (2009) 1715–1723.
[13] E. Martin-Villar, B. Fernandez-Munoz, M. Parsons, et al., Podoplanin associates with CD44 to promote directional cell migration, Mol. Biol. Cell. 21 (2010) 4387–4399.
[14] R. Wadhwa, K. Taira, S.C. Kaul, An Hsp70 family chaperone, mortalin/mthsp70/PBP74/Grp75: what, when, and where?, Cell Stress Chaperones 7 (2002) 309–316
[15] H. Metwaly, S. Maruyama, M. Yamazaki, et al., Parenchymal-stromal switching for extracellular matrix production on invasion of oral squamous cell carcinoma, Hum. Pathol. 43 (2012) 1973–1981.
[16] B. Xu, Y. Zhang, Z. Zhao, et al., Usage of electrostatic eliminator reduces human keratin contamination significantly in gel-based proteomics analysis, J. Proteomics 74 (2011) 1022–1029.

[17] M.C. Bonaccorsi di Patti, R. Miele, M. Eugenia Schinina, et al., The yeast multicopper oxidase Fet3p and the iron permease Ftr1p physically interact, Biochem. Biophys. Res. Commun. 333 (2005) 432–437.
[18] M. Tsuneki, M. Yamazaki, J. Cheng, et al., Combined immunohistochemistry for the differential diagnosis of cystic jaw lesions: its practical use in surgical pathology, Histopathology 57 (2010) 806–813.
[19] E. Martin-Villar, D. Megias, S. Castel, et al., Podoplanin binds ERM proteins to activate RhoA and promote epithelial-mesenchymal transition, J. Cell Sci. 119 (2006) 4541–4553.
[20] A. Kunita, T.G. Kashima, A. Ohazama, et al., Podoplanin is regulated by AP-1 and promotes platelet aggregation and cell migration in osteosarcoma, Am. J. Pathol. 179 (2011) 1041–1049.
[21] V. Schacht, S.S. Dadras, L.A. Johnson, et al., Up-regulation of the lymphatic marker podoplanin, a mucin-type transmembrane glycoprotein, in human squamous cell carcinomas and germ cell tumors, Am. J. Pathol. 166 (2005) 913–921.
[22] P. Yuan, S. Temam, A. El-Naggar, et al., Overexpression of podoplanin in oral cancer and its association with poor clinical outcome, Cancer 107 (2006) 563–569.
[23] H. Kawaguchi, A.K. El-Naggar, V. Papadimitrakopoulou, et al., Podoplanin: a novel marker for oral cancer risk in patients with oral premalignancy, J. Clin. Oncol. 26 (2008) 354–360.
[24] M. Kreppel, M. Scheer, U. Drebber, et al., Impact of podoplanin expression in oral squamous cell carcinoma: clinical and histopathologic correlations, Virchows Arch. 456 (2010) 473–482.
[25] T. Ikarashi, H. Ida-Yonemochi, K. Ohshiro, et al., Intraepithelial expression of perlecan, a basement membrane-type heparan sulfate proteoglycan reflects dysplastic changes of the oral mucosal epithelium, J. Oral Pathol. Med. 33 (2004) 87–95.
[26] R. Wadhwa, S.C. Kaul, Y. Ikawa, et al., Identification of a novel member of mouse hsp70 family. Its association with cellular mortal phenotype, J. Biol. Chem. 268 (1993) 6615–6621.
[27] S.Z. Domanico, D.C. Denagel, J.N. Dahlseid, et al., Cloning of the gene encoding peptide-binding protein 74 shows that it is a new member of the heat shock protein 70 family, Mol. Cell Biol. 13 (1993) 3598–3610.
[28] T. Bhattacharyya, A.N. Karnezis, S.P. Murphy, et al., Cloning and subcellular localization of human mitochondrial hsp70, J. Biol. Chem. 270 (1995) 1705–1710.
[29] L.A. Mizzen, C. Chang, J.I. Garrels, et al., Identification, characterization, and purification of two mammalian stress proteins present in mitochondria, grp 75, a member of the hsp 70 family and hsp 58, a homolog of the bacterial groEL protein, J. Biol. Chem. 264 (1989) 20664–20675.
[30] R. Wadhwa, S. Takano, K. Kaur, et al., Upregulation of mortalin/mthsp70/Grp75 contributes to human carcinogenesis, Int. J. Cancer 118 (2006) 2973–2980.
[31] S. Takano, R. Wadhwa, Y. Yoshii, et al., Elevated levels of mortalin expression in human brain tumors, Exp. Cell Res. 237 (1997) 38–45.
[32] S.R. Dundas, L.C. Lawrie, P.H. Rooney, et al., Mortalin is over-expressed by colorectal adenocarcinomas and correlates with poor survival, J. Pathol. 205 (2005) 74–81.
[33] X. Yi, J.M. Luk, N.P. Lee, et al., Association of mortalin (HSPA9) with liver cancer metastasis and prediction for early tumor recurrence, Mol. Cell Proteomics 7 (2008) 315–325.
[34] L. Bini, B. Magi, B. Marzocchi, et al., Protein expression profiles in human breast ductal carcinoma and histologically normal tissue, Electrophoresis 18 (1997) 2832–2841.
[35] S.S. Mambula, M.A. Stevenson, K. Ogawa, et al., Mechanisms for Hsp70 secretion: crossing membranes without a leader, Methods 43 (2007) 168–175.
[36] S.S. Mambula, S.K. Calderwood, Heat shock protein 70 is secreted from tumor cells by a nonclassical pathway involving lysosomal endosomes, J. Immunol. 177 (2006) 7849–7857.
[37] G. Multhoff, Heat shock protein 70 (Hsp70): membrane location, export and immunological relevance, Methods 43 (2007) 229–237.